Molecular dynamics simulation of imidazolium-based ionic liquids. II. Transport coefficients

ARTICLE *in* THE JOURNAL OF CHEMICAL PHYSICS · JANUARY 2009

Impact Factor: 2.95 · DOI: 10.1063/1.3042279 · Source: PubMed

4 AUTHORS, INCLUDING:

Mohammad H. Kowsari
Institute for Advanced Studies in Basic Scien…
14 PUBLICATIONS **122** CITATIONS
SEE PROFILE

Mahmud Ashrafizaadeh
Isfahan University of Technology
37 PUBLICATIONS **193** CITATIONS
SEE PROFILE

Bijan Najafi
Isfahan University of Technology
43 PUBLICATIONS **781** CITATIONS
SEE PROFILE

Molecular dynamics simulation of imidazolium-based ionic liquids. II. Transport coefficients

M. H. Kowsari,[1] Saman Alavi,[2,a)] Mahmud Ashrafizaadeh,[3] and Bijan Najafi[1]
[1]*Department of Chemistry, Isfahan University of Technology, Isfahan 84156-83111, Iran*
[2]*Department of Chemistry, University of Ottawa, Ottawa, Ontario K1N 6N5, Canada*
[3]*Department of Mechanical Engineering and Supercomputing Center, Isfahan University of Technology, Isfahan 84156-83111, Iran*

(Received 26 September 2008; accepted 16 November 2008; published online 6 January 2009)

A systematic molecular dynamics study is performed to determine the dynamics and transport properties of 12 room-temperature ionic liquids family with 1-alkyl-3-methylimidazolium cation, $[amim]^+$ (alkyl=methyl, ethyl, propyl, and butyl), with counterions, PF_6^-, NO_3^-, and Cl^-. The goal of the work is to provide molecular level understanding of the transport coefficients of these liquids as guidance to experimentalists on choosing anion and cation pairs to match required properties of ionic liquid solvents. In the earlier paper (Part I), we characterized the dynamics of ionic liquids and provided a detailed comparison of the diffusion coefficients for each ion using the Einstein and Green–Kubo formulas. In this second part, other transport properties of imidazolium salts are calculated, in particular, the electrical conductivity is calculated from the Nernst–Einstein and Green–Kubo formulas. The viscosity is also determined from the Stokes–Einstein relation. The results of the calculated transport coefficients are consistent with the previous computational and experimental studies of imidazolium salts. Generally, the simulations give electrical conductivity lower than experiment while the viscosity estimate is higher than experiment. Within the same cation family, the ionic liquids with the NO_3^- counterion have the highest electrical conductivities: $\sigma[NO_3]^- > \sigma[PF_6]^- > \sigma[Cl]^-$. The [dmim][X] series, due to their symmetric cationic structure and good packing and the [bmim][X] series due to higher inductive van der Waals interactions of $[bmim]^+$, have the highest viscosities in these ionic liquid series. Our simulations show that the major factors determining the magnitude of the self-diffusion, electrical conductivity, and viscosity are the geometric shape, ion size, and the delocalization of the ionic charge in the anion. © *2009 American Institute of Physics*. [DOI: 10.1063/1.3042279]

I. INTRODUCTION

Ionic liquids (ILs) are neoteric solvents with remarkable dissolution properties for a wide range of organic, inorganic, organometallic, and polymeric material applications. Their vanishing vapor pressure, very large liquid temperature range, and high thermal stability suggest them as recyclable replacements for traditional volatile organic solvents. ILs with noncoordinating anions can behave as nonreactive solvents. In ILs with coordinating anions, the anion can participate as a ligand or as a cocatalyst in transition metal catalysis.[1] They can also be the key participants for many specific reaction pathways,[2,3] and fundamental elements for enhancing the efficiency of processes that are not possible otherwise using the common molecular solvents. The large electrochemical potential window, high ionic conductivity and mobility, adjustable dielectric constant, and tunable physical and chemical properties make ILs suitable as solvents or inert electrolytes in electrochemical devices, e.g., batteries, fuel cells, double-layer capacitors, and dye-sensitized solar cells.[4–8] Additionally, these solvents have low flammability and are nonvolatile making them safe and robust alternatives for many practical applications under harsh conditions.[9] However, ILs commonly have a high viscosity, which is a major disadvantage in mass transfer, pumping, and mixing processes, and this has limited the electrochemical applications of these salts. Viscosity affects the conductivity and diffusivity of ILs as it strongly affects flow behavior. Many applications and fundamental developments of ILs focus on their use as electrolytes in electrochemistry. Recently, Hapiot and Lagrost[10] published a review about the electrochemical reactivity in room-temperature ILs (RTILs). Below, we discuss the major factors that are important for the selection of a solvent in electrochemical studies.

A primary consideration in the use of an IL in electrochemistry is the electrochemical stability, which is most clearly manifested by the electrochemical potential window or the voltage range over which the solvent is electrochemically inert.[1] In addition to the electrochemical window, the electrical conductivity, σ, which is a measure of the number of the charge carriers (the degree of ion dissociation) and their mobility in the ILs, is critically important. The behavior of ILs as electrolytes is determined by the transport properties of their ionic constituents. Pure ILs possess reasonably good ionic conductivities, which are comparable to the best nonaqueous solvent/electrolyte systems (up to ~ 10 mS cm^{-1}). However, ILs are significantly less conductive than concentrated aqueous electrolytes; for example, the

a)Electronic mail: saman.alavi@nrc-cnrc.gc.ca.

conductivity of aqueous potassium hydroxide (29.4 wt %) solution, used in alkaline batteries, is 540 mS cm^{-1}.[11] Strong ion pairing decreases the number charge carriers in ILs and leads to smaller than expected conductivity.

The IL viscosity is related to the electrical conductivity through Walden's rule, $\Lambda\eta$=const, where Λ is the molar conductivity of the IL ($\Lambda=\sigma M/\rho$). The inverse variation of the conductivity and viscosity in the Walden rule demonstrates that the number of mobile charge carriers in an IL and its viscosity are strongly coupled.[1] In general, reported IL viscosities are two to four orders of magnitude larger than the viscosity of water at room temperature ($\eta[H_2O]=0.89$ cP at 25 °C). A practical method of reducing the viscosity and increasing the electrical conductivity of an IL is the dilution of neat viscous ILs with molecular cosolvents. For example, the conductivity of neat [emim][BF_4] is 14 mS cm^{-1}, while its 2 mol/dm solution in acetonitrile has a conductivity of 47 mS cm^{-1}.[11] This effect has been explained in terms of the solvation and separation of the constituent ions of the IL by the cosolvent molecules. This solvation reduces ion pairing or ion aggregation in the IL, and the number of available charge carriers and the mobility of these charge carriers are increased.[1]

In electrochemical studies of ILs, the ionic diffusion coefficients and the ionic transference numbers are often used to evaluate the transport properties of electrolytes. In our previous study,[12] here after called Part I, we systematically calculated the ionic diffusion coefficients for the 1-alkyl-3-methylimidazolium family of ILs. The ionic diffusion coefficient, D_i (i=cation, anion), is a measure of the rate of motion of an ion in a solution, and the ionic transference number, t_i, is a measure of the fraction of charge carried by that ion in an electric field. The transference numbers measure the relative ability of specific ions (cations or anions) to carry charge. In general, for ILs and especially for imidazolium-based ILs, the cationic transference number is greater than the anionic transference number (see Part I and Ref. 1).

Much progress has been made in the synthesis and application of ILs in chemistry and engineering processes, and systematic studies of their transport properties from the both experiment and theoretical points of view would be timely. A number of experimental studies of the dynamics and transport properties of imidazolium-based ILs were reported in literature.[13–20] Impurities such as water and halide ions have restricted the experimental study of ILs due to their significant effects on the measured physicochemical properties of these salts.[21] ILs are usually hygroscopic and, if exposed to air will to some extent absorb atmospheric moisture.[4] Water impurity in ILs decreases the viscosity and increases both the conductivity and diffusivity. The presence of water also decreases the electrochemical potential window and increases the capacitive current and may lead to the introduction of new electrochemical processes within the potential window.[8] Halide impurity has the opposite effect of water impurity and leads to an increase in viscosity and decrease in electrical conductivity and diffusivity of ILs.

In parallel to experiments, molecular dynamics (MD) simulations and computational modeling are powerful tools for accessing unknown trends and useful properties of ILs. Accurate simulations of the transport properties of ILs are very challenging due to the slow dynamics and high viscosity of these complex liquids. Convergence and reaching the hydrodynamic limit require very large simulation box sizes that are many times beyond current computational capabilities.[22]

In Part II of our study, we continue the modeling of the IL family with 1-alkyl-3-methylimidazolium $[amim]^+$ cation, (alkyl=methyl, ethyl, propyl, and butyl), with counterions, PF_6^-, NO_3^-, and Cl^-. In this study, we systematically calculate and compare the electrical conductivity and the viscosity of imidazolium-based ILs. The effects of the cation and anion structures on the dynamics and transport behavior of the imidazolium-based ILs are studied with identical force fields and simulation parameters instead of individually studying specific cases.

Systematic simulation studies of a series of ILs are rare,[23] especially using explicit all-atom force fields. Due to the large number of atoms and strong Coulombic long-range interactions,[24] long simulation times are needed for computing the dynamics and transport properties in each IL salt and these simulations become costly and require high-performance parallel computing.

In Part I,[12] we summarized earlier MD simulations of dynamics and diffusion coefficients of imidazolium-based ILs. Most previous computational studies focused on the individual members of this family of RTILs. In the following, we briefly discuss MD simulations for computing the electrical conductivities and viscosities of imidazolium-based ILs. For further details, the reader is referred to Part I.

Yan *et al.*[25] calculated the structural and transport properties of [emim][NO_3] at 400 K with polarizable and nonpolarizable electrostatic models. They used momentum fluctuations and transverse-current autocorrelation functions to compute the viscosity from an equilibrium MD simulation. They observed that including polarizability in the potential increased the calculated diffusion coefficients and mobilities and substantially decreased the viscosity of the ions compared to values calculated with a nonpolarizable (fixed charge) model. The polarizable model results were in better agreement with the experimental values and Yan *et al.*[25] concluded that inclusion of polarizability effects in the force field is necessary to properly capture charge screening in ILs. However, recent simulation results indicate that the added realism of a polarizable force field may not be essential for obtaining accurate thermodynamic and transport properties.[26,27]

Lee *et al.*[28] calculated the ionic conductivity of the [bmim][X] salts using the self-diffusion coefficients and employing the Nernst–Einstein relation; see Eq. (4). The calculated ionic conductivities accurately reproduce the experimental trend, $\sigma[C_4F_9SO_3]^- < \sigma[C_3F_7COO]^- < \sigma[PF_6]^- < \sigma[CF_3COO]^- < \sigma[CF_3SO_3]^-$, demonstrating that the self-diffusion coefficient is a major factor in determining the ionic conductivity of ILs.

Bhargava and Balasubramanian[29] calculated transport properties, including the self-diffusion coefficient, shear viscosity, and electrical conductivity of [dmim][Cl] at 425 K

using the all-atom force field developed by Canongia Lopes *et al.*[30] The electrical conductivity was calculated using both the Green–Kubo (0.0089 S cm^{-1}) and Nernst–Einstein (0.012 S cm^{-1}) relations. The electrical conductivity calculated from the Nernst–Einstein relation neglects the cross-correlation terms between the cationic and anionic currents and was calculated to be ~33% higher than the value obtained from the Green–Kubo relation. The calculated electrical conductivity for [dmim][Cl] is low compared to the experimental value of $\sigma_{expt}=0.106$ S cm^{-1}.[31] In comparison to experiments, this potential model predicts a rather large value for the shear viscosity, $\eta_{calc}=0.048$ Pa s. The experimental value of the shear viscosity of [emim][Cl] at 425 K is $\eta_{expt}=0.018$ Pa s and the viscosity for [dmim][Cl] is likely lower than this value because of the molecular symmetry and higher melting point of [dmim][Cl].[29]

In 2006–2007, Rey-Castro *et al.*[32] studied the effect of the rigid model force field of Shim *et al.*[33] and the flexible model force field of Urahata and Ribeiro[34] on the properties of [emim][Cl] and determined the influence of the anion type on the structural and transport properties of [emim][Cl], [emim][NO_3], and [emim][PF_6]. The flexible model of Urahata and Ribeiro[34] leads to an estimate of the viscosity in excellent agreement with extrapolated experimental results. Rey-Castro *et al.*[32] also obtained the stress tensor and the distinct van Hove correlation functions, which indicate that the dynamics of the local structure of the fluid relaxes faster in the flexible model.

Picálek and Kolafa[35] performed a series of MD simulations on [bmim][BF_4], [bmim][PF_6], and [emim][PF_6] using five different force fields.[30,34,36–38] They reported the effect of force field type on the calculated transport properties of the [bmim][PF_6], and their results show the importance of the force field on these properties. They determined the ratio between the ionic conductivity calculated using the Green–Kubo formula, σ_{GK}, and the ionic conductivity from the diffusion coefficients of independent ions assuming Nernst–Einstein relation (Kohlrausch law),[39] σ_{KI}, lies in the range $0.5<\sigma/\sigma_{KI}<0.8$. They concluded that there are only moderate correlations in the ionic motion, and no pronounced clustering of the ions occurs.

From viewing the literature, it becomes apparent that investigations of correlations between chemical structure and transport properties of ILs are relatively rare and details in this area are still not completely understood. Understanding the microscopic dynamics of ILs is necessary for better determining of chemical reactivity, conductivity, interfacial and mixing behaviors, mass transfer, and rheological properties of these compounds. The dynamical and transport properties will also play a major role in determining the performance of ILs in the practical applications, for instance, alternative industrial solvents, analysis of reaction kinetics, separations, lubrications, and electrochemical devices. While a vast number of ILs can be formed by combining different cations and anions, the transport properties of these materials vary widely depending on the type of ions. Thus, the demand for more detailed descriptions of structure/property correlations of ILs increases. If correlations between the chemical structure and transport properties of the ions can be determined, we will be able to design new ILs and to optimize these compounds for specific applications.

In Part I,[12] the dynamics of the ILs are characterized by computing the velocity autocorrelation function (VACF) and the mean-square displacement (MSD) for the centers of mass of the ions at 400 K. The trajectory-averaging technique[40] was employed to evaluate the diffusion coefficients at two temperatures from the linear slope of MSD(t) functions in the range 150–300 ps and from the integration of the VACF(t) functions with upper time limits between 10 and 25 ps at 400 K. Detailed comparisons are made between the diffusion results from the MSD and VACF methods, and cationic transference numbers were estimated from the ionic diffusion coefficients. Finally, we discussed the effect of the cation and anion structures on the dynamic behavior and diffusion coefficients of the imidazolium salts.[12]

In this second part of our work, we report the electrical conductivities and viscosities for the ILs calculated using the Nernst–Einstein and Stokes–Einstein equations, respectively. The electric-current autocorrelation functions are also employed to evaluate the electrical conductivities by the Green–Kubo relation and the cross-correlation terms in the electric-current autocorrelation functions are analyzed.

This paper is organized as follow: In Sec. II simulation details and the methodology applied to calculate the transport properties for 1-alkyl-3-methylimidazolium-based ILs are defined and represented. In Sec. III the results of the MD simulations are presented and discussed. The paper ends with a summary and conclusions in Sec. IV.

II. COMPUTATIONAL METHODS

The simulations were performed with an explicit fully flexible, all-atom force field developed by Canongia Lopes *et al.*[30] for dialkylimidazolium salts based on the OPLS and AMBER framework with some minor modifications. Further details of the force field are given in Part I and are not repeated here.

MD simulations are used to study the 12 1-alkyl-3-methylimidazolium-based ILs (alkyl=methyl, ethyl, propyl, and butyl, with counterions, PF_6^-, NO_3^-, and Cl^-) consisting of 150–294 ion pairs. The simulations are initially performed in the NpT ensemble at $p=1$ atm and $T=400$ K with the modified Nosé–Hoover thermostat/barostat algorithm[41–43] as implemented in the DL_POLY program[44] version 2.15. The thermostat and barostat relaxation times are 0.1 and 2.0 ps, respectively. Periodic boundary conditions were employed and the equations of motion were integrated using the Verlet leapfrog scheme[40] with a time step of 1 fs. All interatomic interactions between the atoms in the simulation box and the nearest image sites were calculated within a cutoff distance of $R_{cutoff}=13.5$ Å for all simulated systems. The electrostatic long-range interactions were calculated using the Ewald summation method[40,45] with a precision of 1×10^{-6}. Each system was equilibrated with a set of 14 runs in the NpT ensemble as mentioned in Part I. By the end of the equilibration, total energies and volumes were monitored until the corresponding time series were stationary. We used an

ensemble-averaging technique to calculate the electric-current autocorrelation functions. The final results were obtained by averaging results from ten 55 ps runs in the *NVE* ensemble. The initial configurations for these *NVE* simulations were obtained from the long runs used to determine the MSDs in our earlier work. Other computational details have been reported in Part I of our work.

The electrical conductivity per unit volume, σ, is defined as the time integral of the electric-current function from the Green–Kubo relation,[46,47]

$$\sigma = \frac{1}{3k_B TV}\int_0^\infty \langle \mathbf{j}(t)\cdot\mathbf{j}(0)\rangle \mathrm{d}t, \tag{1}$$

where the electric-current function $\mathbf{j}(t)$ is defined by

$$\mathbf{j}(t) = \sum_{i=1}^{N} q_i \mathbf{v}_i^c(t) \tag{2}$$

and q_i represents the charge and $\mathbf{v}_i^c(t)$ is the center of mass velocity of ion i. For ILs, the electric-current autocorrelation function $J(t)$ may be written explicitly as[48]

$$J(t) = \sum_{i=1}^{N}\sum_{j=1}^{N}\langle q_i q_j \mathbf{v}_i^c(t)\cdot\mathbf{v}_j^c(t)\rangle = Z(t) + \sum_{i=1}^{N}\sum_{j\neq i}^{N}\langle q_i q_j \mathbf{v}_i^c(t)\cdot\mathbf{v}_j^c(t)\rangle = Z(t)+\Delta(t). \tag{3}$$

The electric-current autocorrelation function is defined as a sum of self, $Z(t)$, and cross terms, $\Delta(t)$. The self-term is the total VACF and the cross term, $J(t)-Z(t)$, indicates the deviation from the ideal Nernst–Einstein behavior and is a measure of the ion-pair formation in the IL.

The Nernst–Einstein equation considers the electrical conductivity to be proportional to the weighted sum of the separate ionic diffusion coefficients,[47]

$$\sigma = \frac{e^2}{kT}\sum_{i=1}^{N}\rho_i q_i^2 D_i. \tag{4}$$

In this relation, e is the electric charge unit, $1.602\,19 \times 10^{-19}$ C, and ρ_i is the density of species i. In the Nernst–Einstein equation the cross term, $\Delta(t)$, is assumed zero. For a 1:1 IL, such as those of interest to this study, the number densities of the cations and anions are equal to the number density of the salt, $\rho = N/V$. The Nernst–Einstein equation can therefore be written as

$$\sigma = \frac{e^2\rho}{kT}\sum_{i=1}^{N} D_i, \tag{5}$$

where the summation is over the cation and the anion diffusion coefficients. According to the Nernst–Einstein equation, the electrical conductivity is proportional to the ionic diffusion coefficients and the mechanism of the charge transport in the ILs is related to the diffusivity of the ions. The reasonable accuracy of the Nernst–Einstein equation for predicting the electrical conductivity of imidazolium-based ILs was investigated in previous studies.[28,32,49] The electrical conductivity is affected by the degree of ion dissociation and inversely related to the magnitude of interionic interactions.[50]

The viscosity, η, of an IL has a strong effect on the flow behavior and the rate of mass transport within a reaction medium or solution. The viscosity is a major input for simulation and optimization of processes in engineering design and analysis. In their roles as solvents, ILs with low viscosity are generally desirable, while when used as lubricants, higher viscosities may be required.[26] Viscosity can be evaluated computationally from both the Green–Kubo and Stokes–Einstein formulas. In the Green–Kubo method, the viscosity is calculated from the time integral over the stress autocorrelation function,[51]

$$\eta = \frac{1}{Vk_B T}\int_0^\infty \langle P_{\alpha\beta}(t)P_{\alpha\beta}(0)\rangle \mathrm{d}t, \tag{6}$$

where each element of the microscopic stress tensor, $P_{\alpha\beta}(t)$, is calculated from the simulation data using[51]

$$P_{\alpha\beta}(t) = \sum_{i=1}^{N}\left[m_i v_{\alpha i} v_{\beta i} + \frac{1}{2}\sum_{i\neq j} r_{\alpha ij} f_{\beta ij}\right], \tag{7}$$

where m_i is the mass of particle i, $v_{\alpha i}$ is the α-Cartesian component of the velocity, $r_{\alpha ij}$ is the α-component of the vector $\mathbf{r}_{ij}$ separating particles i and j, and $f_{\beta ij}$ is the β-Cartesian component of the force between these particles. Due to the force term, the components of the microscopic stress tensor, $P_{\alpha\beta}(t)$, are collective correlation functions which depend on the accumulated contributions from all particles in the system. Consequently, the statistical precision of the calculated viscosity values cannot be improved by simply averaging over all particles in the system. Generally, obtaining good statistics in the calculation of viscosity from the Green–Kubo relation, Eq. (6), requires averaging over very long time trajectories ($\sim$10 ns) to ensure that the integrand has decayed sufficiently to allow the upper limit on the integral to be truncated. As a result, the Green–Kubo method is difficult to apply in simulations of highly viscous ILs since the correlation function converges very slowly with time.[52,53]

Alternatively, the diffusion coefficient is often used to estimate the values of the viscosity by the Stokes–Einstein equation

$$D_i = \frac{k_B T}{c\pi\eta r_{s,i}}, \tag{8}$$

where c is a constant, and $r_{s,i}$ is the effective hydrodynamic (Stokes) radius of the ion i. The effective radius, r_s, for the $[\mathrm{amim}]^+$ and PF_6^- ions have been obtained from the MM2 and *ab initio* molecular orbital calculations.[54] The Stokes–Einstein law is based on a hydrodynamic model that assumes each ion is a sphere moving through a continuum solvent medium. The value of c depends on the nature of the system and the interactions experienced by the solute. For large molecular solutes in small solvent environments, c can be as high as 6. As the solute and solvent become more similar in size, especially in higher viscous liquids, the value of c is reduced to $\sim$4. Thus, the factor c may help to characterize the microscopic ion dynamics in the RTILs.[17,18]

Tokuda *et al.*[17,18] experimentally showed a good linear relationship between D_i and $T\eta^{-1}$ for the cationic diffusion

TABLE I. The electrical conductivity from the Nernst–Einstein relation, σ_{NE} (10^{-3} S cm^{-1}), the electrical conductivity from the Green–Kubo relation, σ_{GK} (10^{-3} S cm^{-1}), and the viscosity from the Stokes–Einstein relation, η (mPa s), for 12 ILs at $T=400$ K. The ionic diffusion coefficients used in calculating σ_{NE} and η are reported in Part I.[12]

	σ_{NE}				η	
IL ([amim][X])	MSD	VACF	σ_{GK}	$\frac{\sigma_{GK}}{\sigma_{NE}(VACF)}$	MSD	VACF
[dmim][Cl]	5.7	13.3	4.6	0.35	104.9	52.4
[dmim][NO_3]	19.3	29.6	12.2	0.41	32.4	21.3
[dmim][PF_6]	10.3	17.8	16.0	0.90	41.5	23.3
[emim][Cl]	13.8	23.1	15.8	0.68	38.4	25.7
[emim][NO_3]	24.4	35.0	23.4	0.67	21.5	15.6
[emim][PF_6]	14.1	20.2	10.9	0.54	25.3	18.5
[pmim][Cl]	8.8	18.7	10.0	0.53	52.8	28.2
[pmim][NO_3]	16.5	28.8	17.8	0.62	27.7	16.9
[pmim][PF_6]	10.2	12.7	10.9	0.86	29.2	27.7
[bmim][Cl]	2.5	9.2	4.9	0.53	182.2	53.1
[bmim][NO_3]	14.6	16.4	6.7	0.41	27.9	24.2
[bmim][PF_6]	9.7	13.2	12.4	0.94	28.8	22.6

coefficients in [amim][$(CF_3SO_2)_2N$] and [bmim][X] ILs, with all lines passing through the origin. This observation indicates that the ionic diffusivity in the ILs basically obeys Eq. (8) and that the viscosity of the solution is the predominant factor in determining the diffusion of the ionic species in ILs. However, fractional Stokes–Einstein relation, $D_i \propto (T/\eta)^{\beta}$ with $\beta \approx 0.8-0.9$, is used in some recent studies for describing the relationship between the diffusion and viscosity in RTILs.[55–58] In our calculations, we will estimate the viscosity using the Stokes–Einstein relation based on the cation diffusion coefficients and $c=4$ for all cases.

III. RESULTS AND DISCUSSION

A. Electrical conductivities

We calculated the electrical conductivity from both the Green–Kubo relation, Eq. (1), and the Nernst–Einstein equation, Eq. (4). The diffusion coefficients from the slopes of MSD plots and from the integration of the VACFs in Part I were used to calculate the electrical conductivities from the Nernst–Einstein equation. The results of the electrical conductivity at 400 K, given in Table I, are calculated to be in the range $10^{-3}-10^{-2}$ S cm^{-1}. This range is consistent with other computational and experimental studies of imidazolium salts.[11] These conductivities are relatively large and this may be due to the free space in the imidazolium ILs, which reduces the effective friction for the planar cations relative to that of for the anions. The motion of the cation parallel to the imidazolium ring has a smaller effective radius than the motion perpendicular to the ring.[59] This large anisotropic translational motion of the imidazolium cation, rather than its large molecular size, may be the source of the good charge carrier properties of the cation.

The influence of the length of the alkyl chain on the cations and the effect of the shape, size, and mass of the anions on the computed electrical conductivities can also be observed (see Table I). In good agreement with experiment, increasing the length of the alkyl chain side in the imidazolium cation decreases the electrical conductivity of the IL.[60] This is due to the more hindered motion of the cations with the longer alkyl side chains. The longer alkyl chains also lead to an increase in the viscosity of the ILs due to stronger interionic van der Waals (vdW) interactions, which increase the ion association in the ILs, see below. In agreement with experiments,[14,17] in the series of imidazolium cations, $[dmim]^+$ has a relatively higher electrical conductivity. The reported experimental trends for the diffusion and inverse viscosity of ILs with the same anion are $[emim]^+ \geq [dmim]^+ > [bmim]^+ > [C_6mim]^+ > [C_8mim]^+$ and the trends for electrical conductivity are similar with one difference: $\sigma[dmim]^+ \geq \sigma[emim]^+ > \sigma[bmim]^+ > \sigma[C_6mim]^+ > \sigma[C_8mim]^+$.[17] Tokuda *et al.*[17] ascribed the high electrical conductivity of [dmim][$(CF_3SO_2)_2N$] (up to 10^{-2} S cm^{-1}), despite lower ionic diffusion coefficients and higher viscosity than that of $[emim]^+$ based liquids, to its high molar concentration of charge carriers (density). The $[dmim]^+$ salt also shows the highest electrical conductivity among [amim][$N(CN)_2$] IL series with the trend $\sigma[dmim]^+ > \sigma[emim]^+ > \sigma[bmim]^+ > \sigma[C_6mim]^+$.[61] In another experimental study, Vila *et al.*[62] stated that increasing the alkyl chain length limits the movement of the imidazolium cations, and so the ILs with longer alkyl chains have lower electrical conductivities.

In general, within the same cation family in Table I, the ILs with the NO_3^- counterion have the highest Nernst–Einstein electrical conductivities: $\sigma[NO_3]^- > \sigma[PF_6]^- > \sigma[Cl]^-$. The same trend is observed for the diffusion coefficients in Part I. The anion size has two opposite effects in the electrical conductivity. On the one hand, the large anions have a smaller surface electrical charge density and thus higher ionic mobility. On the other hand, the larger size of the anion limits the dynamical movement and decreases the

electrical conductivity.[62] From another viewpoint, the smaller anions are better packed in the liquid phase, which may limit their motion. The NO_3^- has a larger anion size but a lower surface electrical charge density than the Cl^-. The NO_3^- has a smaller anion size (and mass) and consequently greater mobility than PF_6^-. Therefore, the NO_3^- has the highest electrical conductivity between the anion species from our results (see Table I) and the [emim][NO_3] can be characterized as the best charge carrier. From experimental work on [bmim][X], Rivera *et al.*[63] observed that ILs with the PF_6^- counterion have higher electrical conductivity compared to those with the Cl^- counterion. The experimental trend of σ in their work is σ[bmim][$(CF_3SO_2)_2N$] $>\sigma$[bmim][CF_3SO_3] $>\sigma$[bmim][PF_6] $>\sigma$[bmim][Cl].[63] A similar trend for electrical conductivity and viscosity of ILs was observed by Tochigi and Yamamoto[64] using a QSPR model. The ILs with the Cl^- counterions have the smallest electrical conductivity and the highest viscosity.

The comparison of the calculated Nernst–Einstein electrical conductivities indicates that diffusion coefficients from the slope of MSD curves give lower electrical conductivities compared to diffusion coefficients from the integration of VACFs. It seems that the electrical conductivity values from the VACF diffusion coefficients are in better agreement with the limited experimental evidence available. For example, σ_{expt}[emim][Cl]=50.1 mS cm^{-1} at 398 K,[62] whereas we get σ_{NE}(MSD)=13.8 mS cm^{-1} and σ_{NE}(VACF)=23.1 mS cm^{-1}. Similarly, σ_{expt}[emim][PF_6] =54.1 mS cm^{-1} at 398 K,[62] while we get σ_{NE}(MSD) =14.1 mS cm^{-1} and σ_{NE}(VACF)=20.2 mS cm^{-1}.

The electrical conductivity from the Green–Kubo relation is calculated by integrating the electric-current autocorrelation function, Eq. (3). We employed an ensemble-averaging technique to obtain the average electric-current autocorrelation functions from the ten short runs, each of 55 ps, for the IL in the *NVE* ensemble. The average electric-current autocorrelation functions were integrated with upper time limits in the interval between 10 and 25 ps and the electrical conductivity was calculated by averaging these integration results. The general appearance of the electric-current autocorrelation functions and its time integral are shown in Fig. 1 for the [dmim][X] family of ILs.

The Green–Kubo electrical conductivity results, reported in Table I, generally show the same trends observed from the Nernst–Einstein electrical conductivities. The Nernst–Einstein equation assumes no ionic association and unit activity for each ion.[16] As expected, the electrical conductivities calculated from the Green–Kubo integral are lower than the Nernst–Einstein electrical conductivities determined with diffusion coefficient from integration of the VACFs. Numerical errors in integration of the electric-current autocorrelation functions are significant due to the oscillating behavior of this function. We must compare the Green–Kubo electrical conductivities with the corresponding Nernst–Einstein values from VACF diffusion coefficients, which have similar numerical uncertainties. The σ_{GK}/σ_{NE} ratio is in the range 0.35–0.94 for the ILs in this study (see Table I), which shows a broad range of ion association in this family of ILs. To a good approximation, the σ_{GK}/σ_{NE} ratio follows the trends:

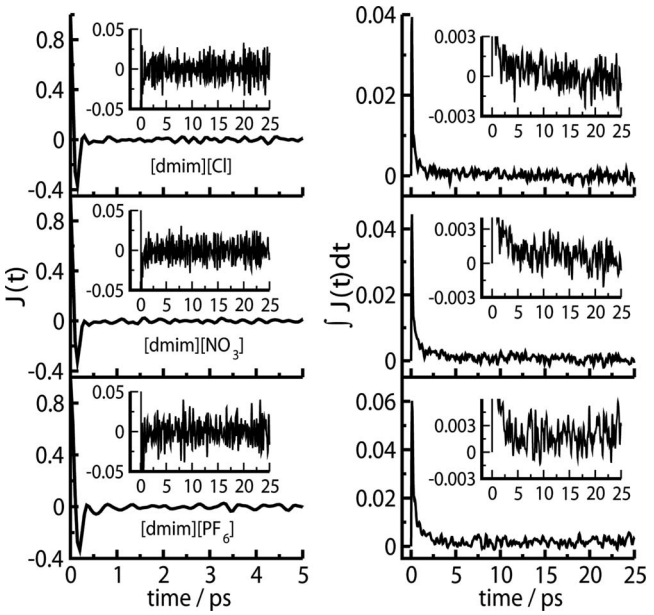

FIG. 1. The calculated normalized electric-current autocorrelation functions (left). The inset shows the magnified long-time behavior of these autocorrelation functions. The integrations of the electric-current autocorrelation functions are shown on the right. The inset shows the magnified long-time behavior of these integrals.

$PF_6^- > NO_3^- \geq Cl^-$. The ILs with PF_6^- counterions have relatively small long-time ion-pair association between cations and anions. Urahata and Ribeiro[65] calculated the electrical conductivity for [bmim][Cl] at 400 K as σ_{NE}=8 mS cm^{-1}, while the σ_{GK} was estimated to be of the order of 10^{-5} S cm^{-1}. Our results for [bmim][Cl] are σ_{NE}(VACF) =9.2 mS cm^{-1} and σ_{GK}=4.9 mS cm^{-1}.

In Fig. 2, we show the electric-current autocorrelation functions, $J(t)$, the total VACFs, $Z(t)$, and the cross terms, $\Delta(t)$, defined in Eq. (3). In all cases, the $J(t)$ have shorter x-intercepts and randomization times than the $Z(t)$ curves.

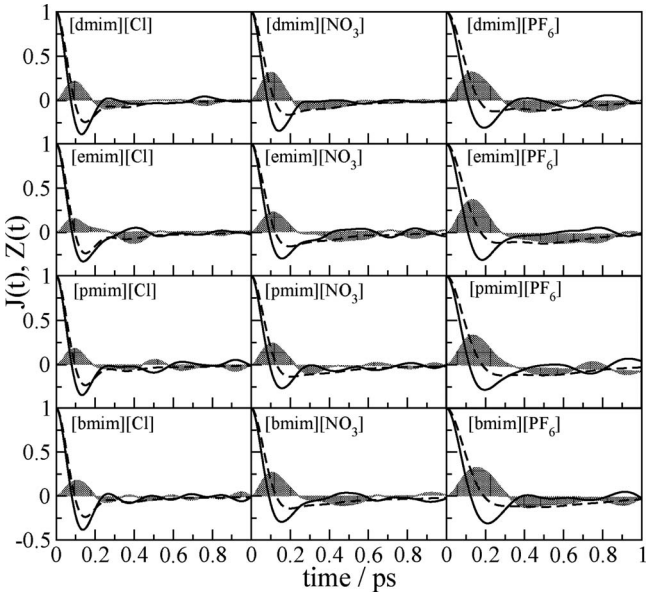

FIG. 2. The calculated normalized electric-current autocorrelation functions (solid lines), total VACFs (dashed lines), and the differences between these two functions (shaded in gray), $[Z(t)-J(t)=-\Delta(t)]$, for 12 ILs at 400 K.

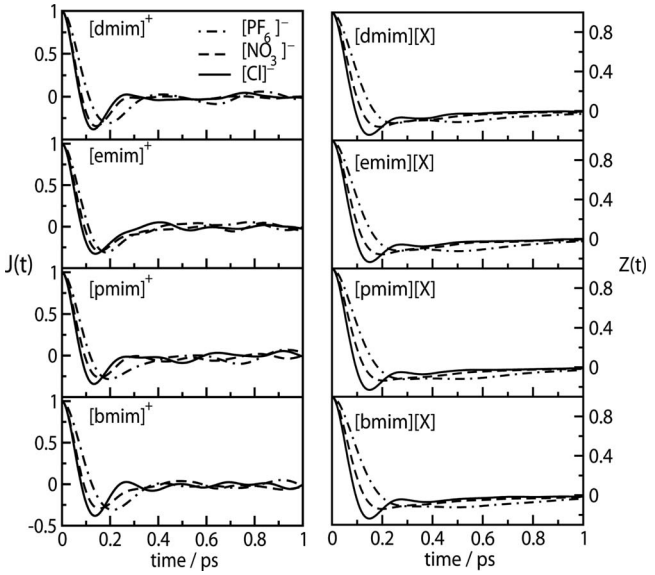

FIG. 3. Comparison of the calculated normalized electric-current autocorrelation, $J(t)$ (left curves), and the total velocity autocorrelation, $Z(t)$ (right curves), at 400 K of [amim][X] ILs with the same cation.

The height of the maximum of the $-\Delta(t)$ terms for the ILs with identical cations follows the trend $[\text{amim}][\text{PF}_6] > [\text{amim}][\text{NO}_3] > [\text{amim}][\text{Cl}]$. This shows that the *initial* short-term correlations between the imidazolium cations and PF_6^- are the strongest. This could be due to the larger size and mass of the PF_6^-. We also see in Fig. 2 that the cross-correlation terms for ILs with the same anions and the different cations are very similar, which shows that the cation-anion interaction strengths are mostly independent of the length of the alkyl side chains. The initial positive $-\Delta(t)$ values decay within 0.2–0.3 ps, after which $-\Delta(t)$ becomes negative. The positive values of $-\Delta(t)$ at short times are an indication of the short-lived anion-cation pairing and diffusion. The decay of $\Delta(t)$ shows that these ionic associations are unstable and decay within 0.5 ps.[48]

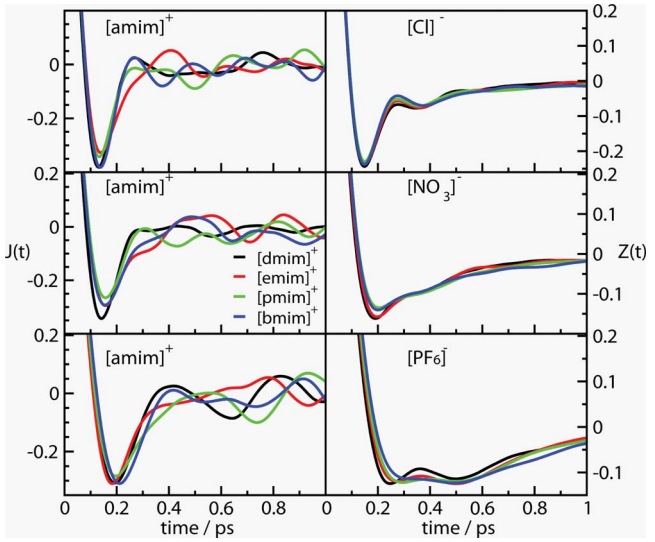

FIG. 4. (Color online) Comparison of the calculated normalized electric-current autocorrelation, $J(t)$ (left curves), and the total velocity autocorrelation, $Z(t)$ (right curves), at 400 K of [amim][X] ILs with the same anion.

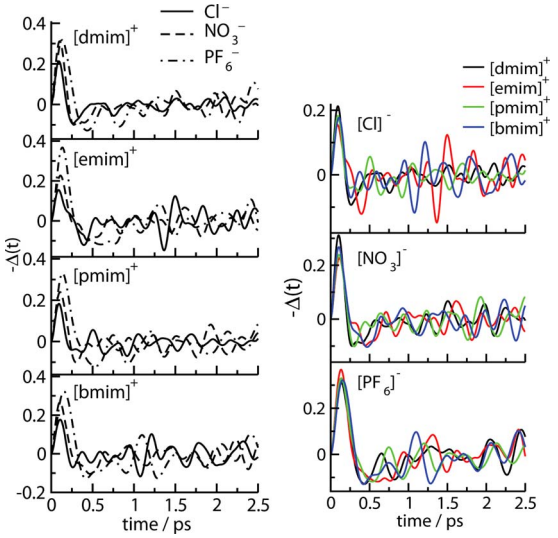

FIG. 5. (Color online) The cross terms, $[Z(t)-J(t)=-\Delta(t)]$, of imidazolium salts with the different anions and the same cations (left), and with the same anions and the different cations (right) at 400 K.

In Fig. 3, the $J(t)$ and $Z(t)$ functions for the $[\text{amim}]^+$ series with different anions are compared. In both cases, the x-intercept and randomization times follow the trend $\text{PF}_6^- > \text{NO}_3^- > \text{Cl}^-$. The decay times for the $J(t)$ curves are seen to be shorter than the corresponding $Z(t)$ curves. In Fig. 4, the $J(t)$ and $Z(t)$ functions for the $[\text{X}]^-$ series with different $[\text{amim}]^+$ cations are compared. In each series, the x-intercepts are virtually identical for the different cations. The order of the total current randomization times for the cations is $[\text{bmim}]^+ > [\text{pmim}]^+ > [\text{emim}]^+ > [\text{dmim}]^+$. For ILs with the lighter anions, the time distance between the x-intercepts in the $J(t)$ and $Z(t)$ plots is shorter.

The analysis of the cross terms, $-\Delta(t)$, for the $[\text{amim}]^+$ series with different anions is shown in Figs. 2 and 5. The magnitudes and times of the first peak of the cross-correlation terms change as $[\text{amim}][\text{PF}_6] > [\text{amim}][\text{NO}_3] > [\text{amim}][\text{Cl}]$. The cross-correlation terms are seen to randomize relatively quickly (at $\sim$1 ps). The $-\Delta(t)$, for the $[\text{X}]^-$ series with different $[\text{amim}]^+$ cations, are shown in Fig. 5. The magnitudes and times of the first peak of the cross-correlation terms are relatively insensitive to the cation alkyl side chain.

In Figs. 2 and 5, the $[\text{amim}][\text{PF}_6]$ ILs have larger positive $-\Delta(t)$ values at short times between 0 and 0.2 ps. This shows that the ion-pair formation in these ILs is strong at short times. However, the $-\Delta(t)$ curves for the $[\text{amim}] \times [\text{PF}_6]$ series also have larger negative regions for time in the range 0.2–1 ps. Time integration over the $-\Delta(t)$ curves for the $[\text{amim}][\text{PF}_6]$ salts gives smaller total values than those of $[\text{amim}][\text{Cl}]$ or $[\text{amim}][\text{NO}_3]$ ILs. Due to the low charge density on the large $[\text{PF}_6]^-$ group, the ion pairs are not long lived, giving large $\sigma_{\text{GK}}/\sigma_{\text{NE}}$ ratios for these salts in Table I. It should be noted that the value of $\sigma_{\text{GK}}/\sigma_{\text{NE}}$ ratio should be considered somewhat independently from the absolute value of the ionic conductivity for an IL.

B. Viscosity

We calculated the viscosity using the Stokes–Einstein equation, Eq. (8). The good accuracy of this equation for ILs has been verified by experimental measurements.[14,17,18] We calculated the viscosity based on the imidazolium *cation diffusion coefficients* and assumed the factor $c=4$ in all cases. This value may not completely illustrate the nature of the dynamics in IL systems but gives a sufficiently good estimation of trends in the viscosities. In reality, the factor c should be increased with increasing alkyl chain length but Tokuda *et al.*[17] showed that c increases only slowly with alkyl chain length in the $[\text{amim}][(CF_3SO_2)_2N]$ series. A rigorous calculation of the viscosity would involve the use of the Green–Kubo relation, Eq. (6).

The values of effective radius, r_s, used for the imidazolium cations in this work from $[\text{dmim}]^+$ to $[\text{bmim}]^+$ are 0.287, 0.303, 0.319, and 0.335 nm, respectively. These radii values are taken from MM2 and *ab initio* molecular orbital calculations of Ue *et al.*[54] for some ILs based on the imidazolium, pyridinium, and ammonium cations. They observed that an increase in the alkyl chain length ($-CH_2-$) of the substituent of the tetraalkylammonium cation causes an increase of about 0.016 nm in the vdW radius of the cation. However, Every *et al.*[14] stated that increasing the alkyl chain length after $[\text{bmim}]^+$ leads to a slight decrease in effective ionic radius before reaching a plateau at $[C_6\text{mim}][\text{I}]$ and $[C_7\text{mim}][\text{I}]$. A possible explanation for this behavior may be that intramolecular interactions between the alkyl chain and the imidazolium ring cause the folding of the long alkyl chain back over the ring. The results of Umecky *et al.*[59] also show that the effective radius increases with the increase in the alkyl chain length, even for alkyl chains much longer than $[\text{bmim}]^+$.[66] More interestingly, Umecky *et al.*[59] observed that the effective radius of anions increases with increasing alkyl chain length from butyl to hexyl and octyl. This is a clear evidence of stronger interionic interactions in the ILs with longer alkyl chain length.[66]

The calculated viscosities in our study for two different temperatures from the Stokes–Einstein equation and using the calculated diffusion coefficients of the imidazolium cations from the Einstein relation are summarized in Tables I and II. Our results give viscosities of imidazolium-based ILs to be in the range 20–200 mPa s at around 400 K, which is consistent with other computational and experimental studies of imidazolium salts.[12,32,67] The influence of the length of the alkyl chain on the cations and the effect of the shape and mass of the anions on the computed viscosities can be observed. The [dmim][X] series have high viscosities due to their symmetric cationic structure and good packing, and the [bmim][X] series have relatively high viscosities due to higher inductive vdW interactions of $[\text{bmim}]^+$. Further, for the same anion, increase in the alkyl chain length from ethyl to butyl results in an increase in the viscosity. Increasing vdW interactions, as well as decreased rotational freedom, are thought to be responsible for the increase in the viscosity.[14] The observed increase in the viscosity with increasing alkyl chain length is in good agreement with previous experimental observations on the imidazolium-based ILs.[14,17,20] The ILs with Cl^- have the highest viscosities in the series of anions, which is opposite to the observed trends in the diffusion coefficients. As expected, the calculated viscosities decrease with temperature.

TABLE II. The number of ion pairs, N, in the simulations, the calculated electrical conductivity from the Nernst–Einstein relation, σ_{NE} (10^{-3} S cm^{-1}), and the viscosity from the Stokes–Einstein relation, η (mPa s), for 12 ILs at several temperatures. The ionic diffusion coefficients for these calculations are from the Einstein relation reported in Part I.

IL ([amim][X])	N	T	σ_{NE}	η
[dmim][Cl]	294	423	10.2	59.9
$[\text{dmim}][NO_3]$	245	383	16.1	37.2
$[\text{dmim}][PF_6]$	216	376	10.2	37.6
[emim][Cl]	252	377	8.7	56.2
$[\text{emim}][NO_3]$	216	379	17.6	27.3
$[\text{emim}][PF_6]$	192	370	9.2	36.7
[pmim][Cl]	216	384	5.6	85.3
$[\text{pmim}][NO_3]$	180	377	14.0	31.5
$[\text{pmim}][PF_6]$	160	373	7.6	38.2
[bmim][Cl]	180	381	1.8	245.0
$[\text{bmim}][NO_3]$	150	379	8.2	48.0
$[\text{bmim}][PF_6]$	150	374	6.4	45.4

The observed trends in the simulated viscosities for the ILs with the same cations are $\eta[\text{amim}][\text{Cl}] > \eta[\text{amim}][PF_6] > \eta[\text{amim}][NO_3]$, as seen in Tables I and II. Our results are in good agreement with other work. For example, Gardas and Coutinho[68] recently estimated the viscosity of some ILs using the group contribution method. They stated that the viscosity of the $[C_n\text{mim}][PF_6]$ increases with the alkyl chain length from 2 to 8. Also, they reported the trends for the viscosity of [amim][X] series as the following for the anion $X: Cl^- > CH_3COO^- > PF_6^- > MeSO_4^- > EtSO_4^- > BF_4^- > CF_3SO_3^- > NTf_2^-$. Gardas and Coutinho[68] stated that the ILs with highly symmetric or almost spherical anions are more viscous.[68] Another comprehensive experimental study of the influence of the nature of the cations and anions on the viscosity, electrical conductivity, and other physical properties of ILs has been reported by Bonhôte *et al.*[50] In their study, anions of the perfluorinated series were used. These anions have strongly delocalized negative charge, which weakens the specific hydrogen bonding interactions with the cation and lowers the viscosity. With a lengthening of the perfluoroalkyl chain, however, the better charge delocalization was largely overcompensated by stronger vdW interactions and viscosity increased.[50]

In Tables I and II, the $[\text{emim}][NO_3]$ IL has the lowest viscosity of the systems studied in this work. The calculated viscosities from the VACF diffusion coefficients are in better agreement with the experimental results. We get $\eta[\text{emim}][\text{Cl}]=25.7$ mPa s (from the VACF) and 38.4 mPa s (from the MSD) and $\eta_{\text{expt}}=8$ mPa s.[21,32,69] Other viscosities calculated for this IL are $\eta[\text{emim}][\text{Cl}]=200$ mPa s (from the VACF)[32] at 400 K using the force field of Shim *et al.*[33] and $\eta[\text{emim}][\text{Cl}]=15$ mPa s at 386 K using the Urahata force

field.[34] For [emim][NO_3], we get η[emim][NO_3] = 15.6 mPa s (from the VACF) and 21.5 mPa s (from the MSD) and η_{expt}=4.42 mPa s.[25,70] Yan *et al.*[25] reported η([emim][NO_3])=6.84 mPa s with a nonpolarized force field and 4.74 mPa s with a polarized force field, and Rey-Castro *et al.*[32] calculated η=193 mPa s (from VACF) using the force field of Shim *et al.*[33]

IV. SUMMARY AND CONCLUSIONS

Transport properties in a set of twelve 1-alkyl-3-methylimidazolium-based ILs are systematically studied by extensive MD simulations using the force field of Canongia Lopes *et al.*[30] Generally, our simulations give diffusion coefficients and electrical conductivities lower than experiment while the viscosity estimates are higher than experiment. Bhargava and Balasubramanian[29] observed similar trends for [dmim][Cl] in their simulations using the force field of Canongia Lopes *et al.*[30] by employing the Einstein relation. The goal of this work is to provide molecular level insight into the factors affecting the values of the transport coefficients in this family of ILs. With a better understanding of structure-property relations, guidelines can be provided for the choice of the proper IL to match the required properties in experimental design.

The major emphasis of the earlier part of this study and perhaps the most important transport property of ILs is the diffusion coefficient. After the diffusion calculations from both of Green–Kubo and Einstein relations in Part I,[12] here we calculated the electrical conductivities from the Nernst–Einstein equation with both sets of calculated diffusion coefficients. The comparison of the calculated Nernst–Einstein electrical conductivities from two diffusion categories (see Table I) indicates that the diffusion coefficients from the slope of MSD curves give lower electrical conductivity values compared to the diffusion coefficients from the integration of VACFs. It seems that the electrical conductivities from the latter are in better agreement with the experiment. The observed general trends for the Nernst–Einstein electrical conductivities from the MSDs and VACFs in Table I are roughly similar. The calculated electrical conductivity in Tables I and II indicates that increasing the length of the alkyl chain side in the imidazolium cation decreases the electrical conductivity of the IL in good agreement with experiment. As expected, motion of the cations with the longer alkyl side chains is more hindered and so the cation with longer side chains contributes less to the electrical conductivity. The longer alkyl chain also leads to an increase in the viscosity of the IL due to stronger interionic vdW interactions, which increase the ion association in the ILs. Within the same cation family in Table I, the ILs with the NO_3^- counterion have the highest Nernst–Einstein electrical conductivities, generally $\sigma[NO_3]^- > \sigma[PF_6]^- > \sigma[Cl]^-$. The anion size has two opposite effects in the electrical conductivity. On the one hand, the large anions have a smaller surface electrical charge density and thus give higher ionic mobility. On the other hand, the larger size of the anion limits the dynamical movement and decreases the electrical conductivity.[62] Our results show that NO_3^- has the highest electrical conductivity and the Cl^- has the lowest electrical conductivity between the anion species. [emim][NO_3] can be used as a good charge carrier.

We also studied the normalized electric-current autocorrelation functions and we calculated the electrical conductivities with the more rigorous Green–Kubo relation by integrating electric-current autocorrelation functions with upper time limits in the range 10–25 ps. In general, the Green–Kubo electrical conductivity results show the same trends observed from the Nernst–Einstein electrical conductivities. As expected, the Green–Kubo relation gives lower values for electrical conductivity than the Nernst–Einstein results from the VACFs in all studied systems. Besides the electric-current autocorrelation functions, the total VACFs and the cross-correlation terms are evaluated and analyzed. In all cases, the electric-current autocorrelation function has shorter *x*-intercept and randomization time than the total VACF curve, and the decay time for the electric-current autocorrelation function curve is seen to be shorter than the corresponding total VACF curve. The magnitudes and times of the first peak of the cross-correlation terms change as [amim][PF_6] > [amim][NO_3] > [amim][Cl] while this first peak is relatively insensitive to the cation alkyl side chain.

Finally, we calculated the Stokes–Einstein viscosities by using two cationic diffusion categories (from the MSD curves and the VACF integrals). The calculated viscosities from the VACF diffusion coefficients are in better agreement with the experimental results.

The [dmim][X] series due to their symmetric cationic structure and good packing and the [bmim][X] series due to higher inductive vdW interactions of $[bmim]^+$ have the highest viscosities in the IL series. Further, for the same anion, increase in the alkyl chain length results from ethyl to butyl in an increase in the viscosity. Increasing vdW interactions, as well as decreasing rotational freedom, is thought to be responsible for the increase in the viscosity.[14] ILs with highly symmetric or almost spherical anions are more viscous. The observed trends in the simulated viscosities for the ILs with the same cations using the diffusion coefficients are η[amim][Cl] > η[amim][PF_6] > η[amim][NO_3]. Thus, the ILs containing planar NO_3^- anions exhibit the lowest viscosities and the ILs with spherical Cl^- counterions exhibit the highest viscosities.

The dynamics and transport properties of RTILs are a combination of the net effect of the electrostatic and the induction interactions (vdW forces) between the ions in the liquid.[17] The major factors determining the magnitude of the transport coefficients are the geometric shape, ion size, and the delocalization of the ionic charge in the anion.

We observed good trends by submitting very long runs for the imidazolium salts and our equilibrium MD results show relatively good agreement with experimental transport coefficients for imidazolium-based ILs.

ACKNOWLEDGMENTS

The computational support for this work by the Supercomputing Center of the Isfahan University of Technology is gratefully acknowledged. M.H.K. thanks Dr. S. J.

Hashemifar for some guidance and acknowledges Mr. Mehdi Rahmani of the Supercomputing Center of Isfahan University of Technology for help on the parallel computing. S.A. would like to thank G. N. Patey and H. V. Spohr for helpful discussions.

[1] P. Wasserscheid and T. Welton, *Ionic Liquids in Synthesis* (Wiley-VCH, Weinheim, 2002).
[2] R. A. Sheldon, R. M. Lau, M. J. Sorgedrager, F. van Rantwijk, and K. R. Seddon, Green Chem. **4**, 147 (2002).
[3] T. Welton, Chem. Rev. (Washington, D.C.) **99**, 2071 (1999).
[4] M. C. Buzzeo, R. G. Evans, and R. G. Compton, ChemPhysChem **5**, 1106 (2004).
[5] R. F. de Souza, J. C. Padilha, R. S. Gonçalves, and J. Dupont, Electrochem. Commun. **5**, 728 (2003).
[6] M. Ue, M. Takeda, A. Toriumi, A. Kominato, R. Hagiwara, and Y. Ito, J. Electrochem. Soc. **150**, A499 (2003).
[7] H. Matsumoto, T. Matsuda, T. Tsuda, R. Hagiwara, Y. Ito, and Y. Miyazaki, Chem. Lett. **30**, 26 (2001).
[8] C. Zhao, G. Burrell, A. A. J. Torriero, F. Separovic, N. F. Dunlop, D. R. MacFarlane, and A. M. Bond, J. Phys. Chem. B **112**, 6923 (2008).
[9] J. F. Brennecke and E. J. Maginn, AIChE J. **47**, 2384 (2001).
[10] P. Hapiot and C. Lagrost, Chem. Rev. (Washington, D.C.) **108**, 2238 (2008).
[11] M. Galiński, A. Lewandowski, and I. Stępniak, Electrochim. Acta **51**, 5567 (2006).
[12] M. H. Kowsari, S. Alavi, M. Ashrafizaadeh, and B. Najafi, J. Chem. Phys. **129**, 224508 (2008).
[13] W. R. Carper, G. J. Mains, B. J. Piersma, S. L. M. Mansfield, and C. K. Larive, J. Phys. Chem. B **100**, 4724 (1996).
[14] H. A. Every, A. G. Bishop, D. R. MacFarlane, G. Orädd, and M. Forsyth, Phys. Chem. Chem. Phys. **6**, 1758 (2004).
[15] C. K. Larive, M. Lin, B. J. Piersma, and W. R. Carper, J. Phys. Chem. B **99**, 12409 (1995).
[16] A. Noda, K. Hayamizu, and M. Watanabe, J. Phys. Chem. B **105**, 4603 (2001).
[17] H. Tokuda, K. Hayamizu, K. Ishii, M. A. B. H. Susan, and M. Watanabe, J. Phys. Chem. B **109**, 6103 (2005).
[18] H. Tokuda, K. Hayamizu, M. A. B. H. Susan, and M. Watanabe, J. Phys. Chem. B **108**, 16593 (2004).
[19] H. Tokuda, K. Ishii, M. A. B. H. Susan, K. Hayamizu, and M. Watanabe, J. Phys. Chem. B **110**, 2833 (2006).
[20] H. Tokuda, S. Tsuzuki, M. A. B. H. Susan, K. Hayamizu, and M. Watanabe, J. Phys. Chem. B **110**, 19593 (2006).
[21] K. R. Seddon, A. Stark, and M. J. Torres, Pure Appl. Chem. **72**, 2275 (2000).
[22] Z. Hu and C. J. Margulis, Acc. Chem. Res. **40**, 1097 (2007).
[23] S. M. Urahata and M. C. C. Ribeiro, J. Chem. Phys. **122**, 024511 (2005).
[24] P. A. Hunt, Mol. Simul. **32**, 1 (2006).
[25] T. Yan, C. J. Burnham, M. G. D. Pópolo, and G. A. Voth, J. Phys. Chem. B **108**, 11877 (2004).
[26] M. S. Kelkar and E. J. Maginn, J. Phys. Chem. B **111**, 4867 (2007).
[27] N. M. Micaelo, A. M. Baptista, and C. M. Soares, J. Phys. Chem. B **110**, 14444 (2006).
[28] S. U. Lee, J. Jung, and Y.-K. Han, Chem. Phys. Lett. **406**, 332 (2005).
[29] B. L. Bhargava and S. Balasubramanian, J. Chem. Phys. **123**, 144505 (2005).
[30] J. N. Canongia Lopes, J. Deschamps, and A. A. H. Pádua, J. Phys. Chem. B **108**, 2038 (2004).
[31] A. A. Fannin, Jr., D. A. Floreani, L. A. King, J. S. Landers, B. J. Piersma, D. J. Stech, R. L. Vaughn, J. S. Wilkes, and J. L. Williams, J. Phys. Chem. **88**, 2614 (1984).
[32] C. Rey-Castro, A. L. Tormo, and L. F. Vega, Fluid Phase Equilib. **256**, 62 (2007).
[33] Y. Shim, M. Y. Choi, and H. J. Kim, J. Chem. Phys. **122**, 044510 (2005).
[34] S. M. Urahata and M. C. C. Ribeiro, J. Chem. Phys. **120**, 1855 (2004).
[35] J. Picálek and J. Kolafa, J. Mol. Liq. **134**, 29 (2007).
[36] C. G. Hanke, S. L. Price, and R. M. Lynden-Bell, Mol. Phys. **99**, 801 (2001).
[37] Z. Liu, S. Huang, and W. Wang, J. Phys. Chem. B **108**, 12978 (2004).
[38] J. K. Shah, J. F. Brennecke, and E. J. Maginn, Green Chem. **4**, 112 (2002).
[39] P. W. Atkins and J. de Paula, *Physical Chemistry*, 8th ed. (Oxford University Press, Oxford, 2006).
[40] M. P. Allen and D. J. Tildesley, *Computer Simulation of Liquids* (Oxford Science, Oxford, 1987).
[41] W. G. Hoover, Phys. Rev. A **31**, 1695 (1985).
[42] S. Melchionna, G. Ciccotti, and B. L. Holian, Mol. Phys. **78**, 533 (1993).
[43] S. Nosé, J. Chem. Phys. **81**, 511 (1984).
[44] W. Smith and T. R. Forester, The DL_POLY molecular simulation package, v. 2.15, Daresbury Laboratory, UK, 2005.
[45] K. D. Gibson and H. A. Scheraga, J. Phys. Chem. B **99**, 3752 (1995).
[46] M. Harada, A. Yamanaka, M. Tanigaki, and Y. Tada, J. Chem. Phys. **76**, 1550 (1982).
[47] J. P. Hansen and I. R. McDonald, *Theory of Simple Liquids* (Academic, New York, 1986).
[48] M. G. Del Pópolo and G. A. Voth, J. Phys. Chem. B **108**, 1744 (2004).
[49] C. Rey-Castro and L. F. Vega, J. Phys. Chem. B **110**, 14426 (2006).
[50] P. Bonhôte, A. Dias, N. Papageorgiou, K. Kalyanasundaram, and M. Grätzel, Inorg. Chem. **35**, 1168 (1996).
[51] J. M. Haile, *Molecular Dynamics Simulation: Elementary Methods* (Wiley, New York, 1992).
[52] W. Jiang, T. Yan, Y. Wang, and G. A. Voth, J. Phys. Chem. B **112**, 3121 (2008).
[53] Z. Hu and C. J. Margulis, J. Phys. Chem. B **111**, 4705 (2007).
[54] M. Ue, J. Electrochem. Soc. **141**, 3336 (1994); M. Ue, A. Murakami, and S. Nakamura, *ibid.* **149**, A1385 (2002).
[55] A. Voronel, E. Veliyulin, and V. Sh. Machavariani, Phys. Rev. Lett. **80**, 2630 (1998).
[56] M. Kanakubo, K. R. Harris, N. Tsuchihashi, K. Ibuki, and M. Ueno, J. Phys. Chem. B **111**, 2062 (2007); K. R. Harris, M. Kanakubo, N. Tsuchihashi, K. Ibuki, and M. Ueno, *ibid.* **112**, 9830 (2008).
[57] H. V. Spohr and G. N. Patey, J. Chem. Phys. **129**, 064517 (2008).
[58] T. Köddermann, R. Ludwig, and D. Paschek, ChemPhysChem **9**, 1851 (2008).
[59] T. Umecky, M. Kanakubo, and Y. Ikushima, Fluid Phase Equilib. **228–229**, 329 (2005).
[60] J. Leys, M. Wübbenhorst, C. P. Menon, R. Rajesh, J. Thoen, C. Glorieux, P. Nockemann, B. Thijs, and K. Binnemans, J. Chem. Phys. **128**, 064509 (2008).
[61] Y. Yoshida, O. Baba, and G. Saito, J. Phys. Chem. B **111**, 4742 (2007).
[62] J. Vila, L. M. Varela, and O. Cabeza, Electrochim. Acta **52**, 7413 (2007).
[63] A. Rivera, A. Brodin, A. Pugachev, and E. A. Rössler, J. Chem. Phys. **126**, 114503 (2007).
[64] K. Tochigi and H. Yamamoto, J. Phys. Chem. C **111**, 15989 (2007).
[65] S. M. Urahata and M. C. C. Ribeiro, J. Chem. Phys. **124**, 074513 (2006).
[66] T. Umecky, M. Kanakubo, and Y. Ikushima, J. Mol. Liq. **119**, 77 (2005).
[67] S. Zhang, N. Sun, X. He, X. Lu, and X. Zhang, J. Phys. Chem. Ref. Data **35**, 1475 (2006).
[68] R. L. Gardas and J. A. P. Coutinho, Fluid Phase Equilib. **266**, 195 (2008).
[69] R. L. Perry, K. M. Jones, W. D. Scott, Q. Liao, and C. L. Hussey, J. Chem. Eng. Data **40**, 615 (1995).
[70] K. R. Seddon, A. Stark, and M.-J. Torres, *Clean Solvents: Alternative Media for Chemical Reactions and Processing*, ACS Symposium Series (American Chemical Society, Washington, DC, 2002).